

# Grau en Matemàtiques

---

**Títol:** Tilings and the Aztec Diamond Theorem

**Autor:** David Pardo Simón

**Director:** Anna de Mier

**Departament:** Mathematics

**Any acadèmic:** 2015-2016





# Tilings and the Aztec Diamond Theorem

A dissertation submitted to the Polytechnic University of Catalonia in accordance with the requirements of the Bachelor's degree in Mathematics in the School of Mathematics and Statistics.

David Pardo Simón

Supervised by Dr. Anna de Mier

School of Mathematics and Statistics

June 28, 2016



# Abstract

Tilings over the plane  $\mathbb{R}^2$  are analysed in this work, making a special focus on the Aztec Diamond Theorem. A review of the most relevant results about monohedral tilings is made to continue later by introducing domino tilings over subsets of  $\mathbb{R}^2$ . Based on previous work made by other mathematicians, a proof of the Aztec Diamond Theorem is presented in full detail by completing the description of a bijection that was not made explicit in the original work.

**MSC2010:** 05B45, 52C20, 05A19.



# Contents

<b>1</b>	<b>Tilings and basic notions</b>	<b>1</b>
1.1	Monohedral tilings . . . . .	3
1.2	The case of the heptiamonds . . . . .	8
1.2.1	Domino Tilings . . . . .	13
<b>2</b>	<b>The Aztec Diamond Theorem</b>	<b>15</b>
2.1	Schröder numbers and Hankel matrices . . . . .	16
2.2	Bijection between tilings and paths . . . . .	19
2.3	Hankel matrices and n-tuples of Schröder paths . . . . .	27



# Chapter 1

## Tilings and basic notions

The history of tilings and patterns goes back thousands of years in time. Human beings started to select shapes and colours to cover the walls and floors of their houses as soon as they began to build them with stone. Everybody knows that mankind has made use of tilings and patterns in a wide range of different styles. For example, the Arabs were specially concerned with using simple shapes and colours to create complex geometric designs, whereas the Greeks and other European cultures preferred using human images and elements copied from nature in their mosaics.

This topic has also been widely studied by mathematicians and, in fact, there are a lot of results related to it. In this paper I am going to introduce the results which I think are most relevant.



Figure 1.1: On the left a Roman Mosaic in The National Museum of Roman Art in Merida. On the right a detail of a tiling from the Alhambra.

A first mathematical definition of such mosaics can be the following: any countable covering of the plane by closed subsets with neither gaps nor overlaps can be considered a *plane tiling*  $\mathcal{T}$ .

However, this definition would be too broad. Thus, in order to exclude some problematic or irrelevant cases to our purposes, we also impose the condition that each tile must be a closed topological disk, which we can consider to be any set whose boundary is a single simple closed curve, that is, a "loop", with no branches or crossings (i.e. any simply-connected domain).

**Definition 1.0.1.** A **plane tiling**  $\mathcal{T}$  is a countable family of closed topological disks  $\mathcal{T} = \{T_1, T_2, \dots\}$ , called **tiles**, which cover the plane without gaps or overlaps (these sets can only intersect in their boundaries). That is, the union of the tiles  $T_1, T_2, \dots$  is the whole plane, and their interiors are pairwise disjoint.

Many important properties of tilings are related to the idea of symmetry. Through the following definitions we will introduce the required background that will be needed in further sections.

**Definition 1.0.2.** An **isometry** is any mapping of the Euclidean plane onto itself which preserves all distances. This can be a rotation, a translation, a reflection or a glide reflection (combination of a reflection in a line and a translation along that line).

A **symmetry** of a set  $T \in \mathbb{R}^2$  is an isometry which maps  $T$  onto itself. For a given set  $T$  we define its **symmetry group** as

$$S(T) = \{ \text{symmetries of } T \},$$

which indeed has the algebraic structure of a group.

By considering the isometries that map each tile to another tile, we can restrict these definitions to tilings instead of general sets, which provides us with new properties and classifications for tilings:

**Definition 1.0.3.** A tiling  $\mathcal{T}$  is said to be **symmetric** if the order of  $S(\mathcal{T})$  is greater than one, that is, it does not consist of the identity alone. In addition,  $\mathcal{T}$  is a **periodic** tiling if  $S(\mathcal{T})$  contains at least two translations in non-parallel directions. (Fig. 1.2).

**Definition 1.0.4.** Let  $\mathcal{T}$  be a tiling and  $T_1, T_2$  two different tiles of  $\mathcal{T}$ ,  $T_1$  and  $T_2$  are **equivalent** if the symmetry group  $S(\mathcal{T})$  contains a transformation that maps

$T_1$  onto  $T_2$ .

The collection of all tiles of  $\mathcal{T}$  that are equivalent to  $T_1$  is called the **transitivity class** of  $T_1$ , and if all tiles of  $\mathcal{T}$  form a single transitivity class we say that  $\mathcal{T}$  is **isohedral**.

**Definition 1.0.5.** A tiling  $\mathcal{T}$  is said to be **normal** if:

- *Every tile of  $\mathcal{T}$  is a topological disk.*
- *The intersection of every two tiles of  $\mathcal{T}$  is a connected set, that is, it does not consist of two (or more) distinct and disjoint parts.*
- *The tiles of  $\mathcal{T}$  are uniformly bounded, in the sense that there exist  $U$  and  $u$  positive numbers such that every tile contains some circular disk of radius  $u$  and is contained in some circular disk of radius  $U$ .*

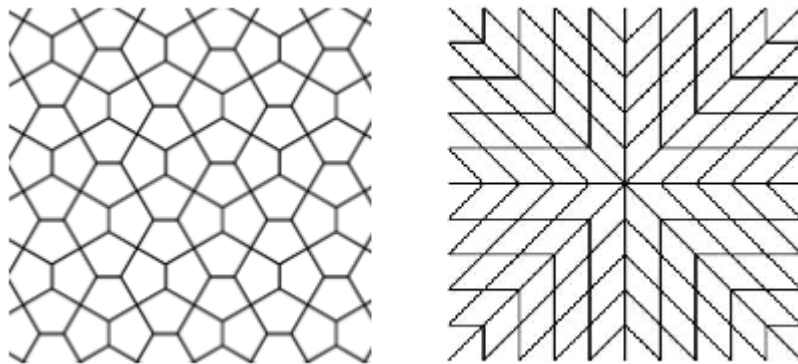


Figure 1.2: On the left, a typical periodic tiling. On the right, a non-periodic tiling.

**Definition 1.0.6.** A normal tiling by polygons  $\mathcal{T}$  is called **proper** if the intersection of any two tiles of  $\mathcal{T}$  is contained in a side of each tile.

## 1.1 Monohedral tilings

After introducing general definitions and characterizations of tilings in the previous section, in this one we focus on those tilings formed by isomorphic tiles:

**Definition 1.1.1.** A **monohedral tiling** is one in which all the tiles are the same shape and size. In such case, its unique (up to isomorphism) tile  $T$  is called the **prototile** of the tiling  $\mathcal{T}$  and we say that the prototile  $T$  admits the tiling  $\mathcal{T}$ .

**Definition 1.1.2.** A monohedral tiling  $T$  is said to be **regular** when tiles are regular polygons and adjacent tiles only share one full side.

It is not possible to construct monohedral regular tilings out of any regular polygon. In fact, there are only three possible prototiles:

**Theorem 1.1.3.** *There exist only three regular monohedral tilings, whose possible prototiles are the equilateral triangle, the square, or the regular hexagon. (fig. 1.3)*

*Proof.* Observe that since a tiling is a countable family of pieces ordered in such a way that there are no gaps left among them, the sum of the angles of the regular polygons congruent in a vertex must be exactly  $360^\circ$ . Besides, the number of pieces that share a vertex is an integer.

Thus, we look at regular polygons whose angles are a divisor of  $360^\circ$ . The only ones satisfying this condition are the regular triangle, square and hexagon ( $60^\circ$ ,  $90^\circ$  and  $120^\circ$  respectively).  $\square$

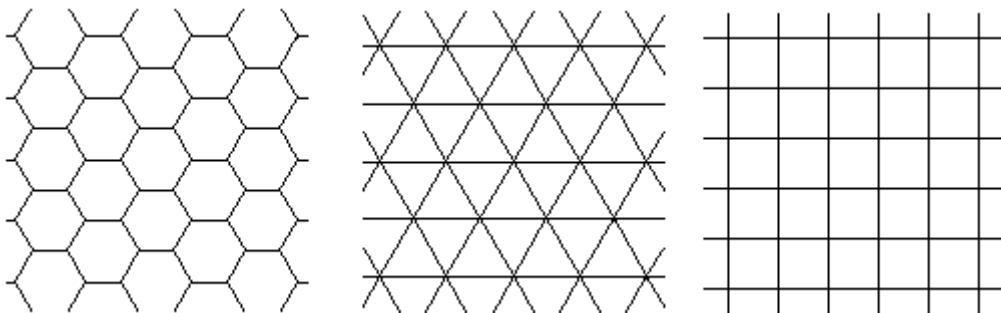


Figure 1.3: The three regular tessellations.

Monohedral tilings may seem a trivial matter, but the reality is far from that. We still lack of an algorithm to determine whether a given set  $T$  is the prototile of a monohedral tiling. And in addition of constructing some easy examples, like the aforementioned ones, we can also consider much more difficult cases, as we will see in the following results and in a further example regarding the heptiamonds.

We will first introduce a classification criteria for polygons, so we can study the number of possible monohedral tilings by polygons.

**Definition 1.1.4.** Two tilings  $\mathcal{T}_1$  and  $\mathcal{T}_2$  are said to be of the same **polygonal isohedral type** if there exists a homeomorphism  $\phi$  that maps the vertices of  $\mathcal{T}_1$

onto those of  $\mathcal{T}_2$  in such a way that a vertex  $V$  of  $\mathcal{T}_1$  is a corner of a tile  $T$  in  $\mathcal{T}_1$  if and only if  $\phi(V)$  is a corner of a tile  $\phi(T)$  in  $\mathcal{T}_2$ .

In other words, every tile  $T$  of  $\mathcal{T}_1$  has the same number of sides as the corresponding tile  $\phi(T)$  of  $\mathcal{T}_2$ , and if any side  $E$  of  $T$  is made up of two or more edges  $E_1, E_2, \dots, E_n$  of  $\mathcal{T}_1$  then the corresponding side  $\phi(E)$  of  $\phi(T)$  is made up of the same number of edges  $\phi(E_1), \phi(E_2), \dots, \phi(E_n)$  of  $\mathcal{T}_2$ .

As stated by Grunbaum and Shephard [5], there exist precisely 107 polygonal isohedral types of proper tilings by convex polygons; of these, 14 types have triangular tiles, 56 types have quadrangular tiles, 24 types have pentagonal tiles and 13 types have hexagonal tiles. There are no other polygonal isohedral tilings by convex tiles; in particular, there are no such tilings by  $n$ -gons with  $n \geq 7$ .

**Definition 1.1.5.** A polygon is said to be **anisohedral** if it admits a monohedral tiling but does not admit any isohedral tiling.

While the problem of finding all the different isohedral monohedral tilings by polygons admits no discussion, a much more complex question arises when we remove the condition of isohedrality. Until 1935 it was generally believed that every polygon which admitted a monohedral tiling also admitted an isohedral tiling. The eighteenth of the twenty-three famous Hilbert's famous problems [7] asked whether there exists an anisohedral tile in a 3-dimensional space. From the context it appears that Hilbert assumed that the corresponding planar problem had no solution. However, he was contradicted by Heesch in 1935 [6], who found a counterexample (see fig. 1.4).

**Theorem 1.1.6.** *All quadrilaterals are the prototile of a monohedral tiling.*

*Proof.* The tiling is formed by rotating the quadrilateral by  $180^\circ$  about the midpoints of its sides. The same process is then applied to the four new quadrilaterals, and so on.

Another approach is noticing that in a quadrilateral the interior angles sum up to  $360^\circ$ , and so in the tiling we just need each vertex to be the joint of the original A, B, C, and D vertices of the quadrilateral (fig. 1.5).

□

**Theorem 1.1.7.** *All triangles are the prototile of a monohedral tiling.*

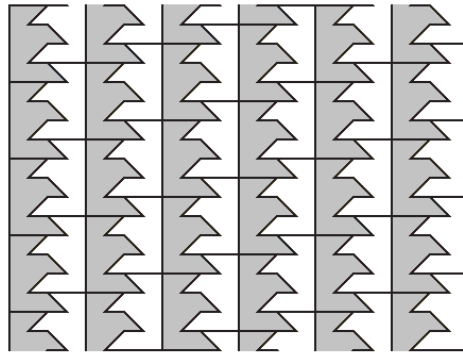


Figure 1.4: A possible tiling with the prototile found by Heesch in 1935. Heesch proved that his prototyle could not tile the plane with only one symmetry class. In the tiling of the picture we can see two different symmetry classes of tiles, represented with grey and white.

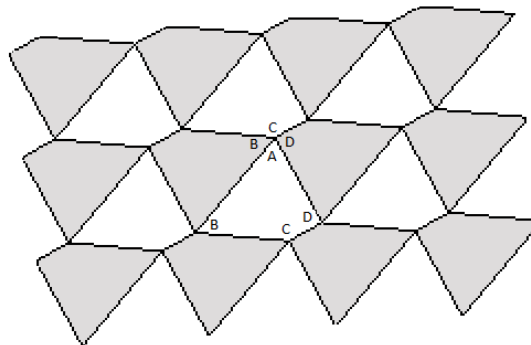


Figure 1.5: An illustrative example of Theorem 1.1.6.

*Proof.* We can join two of the triangles to convert them into a quadrilateral, then the previous result applies.  $\square$

It should be noticed that in the cases of the quadrilaterals we did not need the condition of them to be convex.

We will now consider the case of pentagons, which is slightly different to the previous ones. Fifteen types of convex pentagons are known to be prototiles of monohedral tilings, but there is no proof that this is the total amount. The key is that unlike triangles and quadrilaterals, there exist anisohedral convex pentagons, and some of them are prototiles of possible tilings. The most recent one was discovered in 2015 by a group of three mathematicians from the University of Washington, Bothell (fig. 1.6).

Despite being apparently simple, the problem of finding how many different types

of pentagons tile the plane is almost unsolvable, since there are infinitely many different anisohedral types of pentagons (which does not happen with quadrilaterals or triangles). The current approach involves computation: define an algorithm and let some powerful computer working for a long time with the hope of finding a new different prototile.

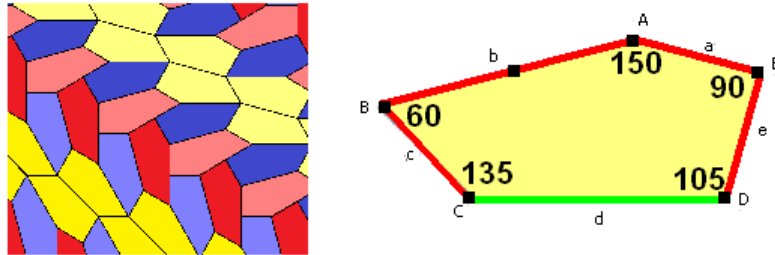


Figure 1.6: The 15th monohedral tiling with a convex anisohedral pentagon as the prototile.

Regarding hexagons, it was proved by Reinhardt [15] that there are no convex anisohedral hexagons. Finally, completing the study of monohedral tilings by polygons, the following was proved by Niven [14]:

**Theorem 1.1.8.** *No convex polygon of more than six sides admits a monohedral tiling of the plane.*

At this point, one could wonder about how non-convex polygons tile the plane. The topic is too deep for the purpose of this paper, so we will only consider some cases here. In particular, the case of polygons formed by joining regular triangles, quadrilaterals, or hexagons.

**Definition 1.1.9.** A **polyiamond** is a topological disk constructed by joining together identical equilateral triangles, taken from the regular tiling by such triangles. An  **$n$ -iamond** is a polyiamond of order  $n$ , that is, formed by  $n$  equilateral triangles. Analogous definitions exist for **polyominoes** (using squares instead of triangles), and **polyhexes** (using regular hexagons).

There are still no known formulae which give the number of polyiamonds, polyominoes or polyhexes as a function of  $n$ , so this remains as an unsolved combinatorial problem nowadays. However, some researchers have determined the first of these numbers empirically (see [10] [11] [2]).

### Application to tilings:

The problem that arises now is to determine which of these polyiamonds, polyominoes and polyhexes are prototiles of a monohedral tiling. An up to date summary of what is known and what is yet unsolved has been compiled by Joseph Myers [13]. Due to the vast amount of different results existing on this kind of polygons, we cannot cover all of them. In this paper we will only consider the case of the *heptyiamonds*, which is of special interest. For this purpose the following criterion will be useful:

**Theorem 1.1.10 (The Conway Criterion.).** *Let  $U$  be a closed topological disk with six consecutive points  $A, B, C, D, E$ , and  $F$  onto the boundary, satisfying the following properties:*

- *the boundary part from  $A$  to  $B$  is congruent by translation to the boundary part from  $E$  to  $D$ .*
- *each of the boundary parts  $BC$ ,  $CD$ ,  $EF$  and  $FA$  is congruent to itself when rotated by  $180^\circ$  around itself.*
- *at least three out of the six points must be distinct.*

*Then  $U$  admits a periodic tiling of the plane and does so using only translation and  $180^\circ$  rotations.*

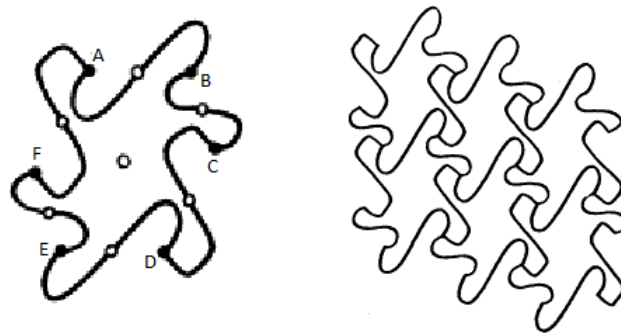


Figure 1.7: A topological disk satisfying Conway's Criterion next to a corresponding tiling.

## 1.2 The case of the heptyiamonds

Out of the 24 heptyiamonds, all of them except the V-shaped one admit a monohedral tiling of the plane (fig. 1.8).

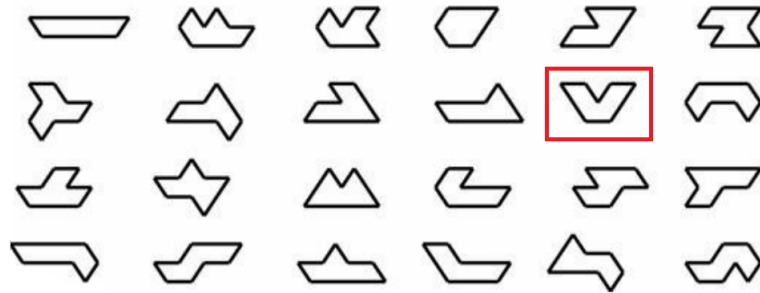


Figure 1.8: The 24 heptiamond with the "special" one surrounded by a red framework.

We will first show why this one is not a prototile of a monohedral tiling:

After placing the first tile (green in the figure), we must fill the concave region  $A$ . For this purpose we have two symmetric possibilities, so we shall only consider one of them, placing this way the second tile (blue)(fig. 1.9).

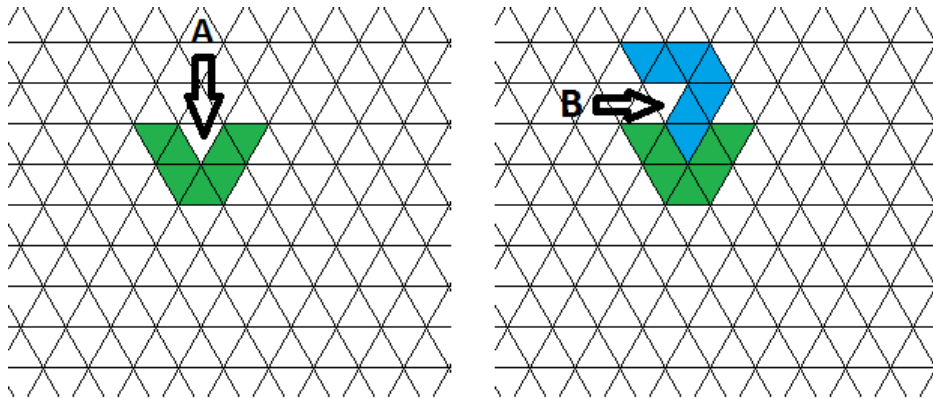


Figure 1.9: First step.

To fill the concave region  $B$  of the second tile there is only one possibility, so we place the third tile (yellow)(fig. 1.10).

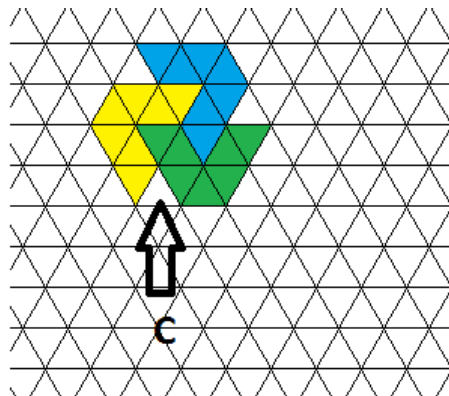


Figure 1.10: Second step.

Now we focus our attention on the empty region between the first and the third tile,  $C$  in the figure. This can be filled in one of two ways with the 4th tile (red). The first possibility immediately leads to a dead end, since there is no way to cover the region  $D$  (fig. 1.11).

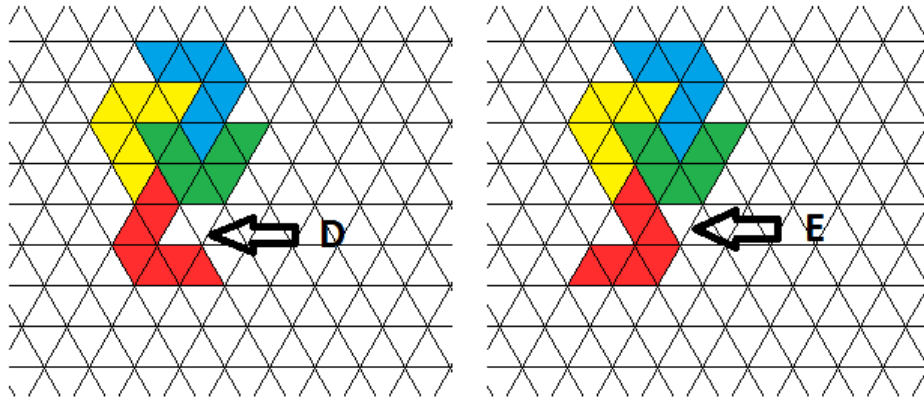


Figure 1.11: Third step.

For the second possibility we have again two new options to cover  $E$  the 5th tile (grey), both leading to regions that could not be covered ( $F$  and  $G$ )(fig. 1.12).

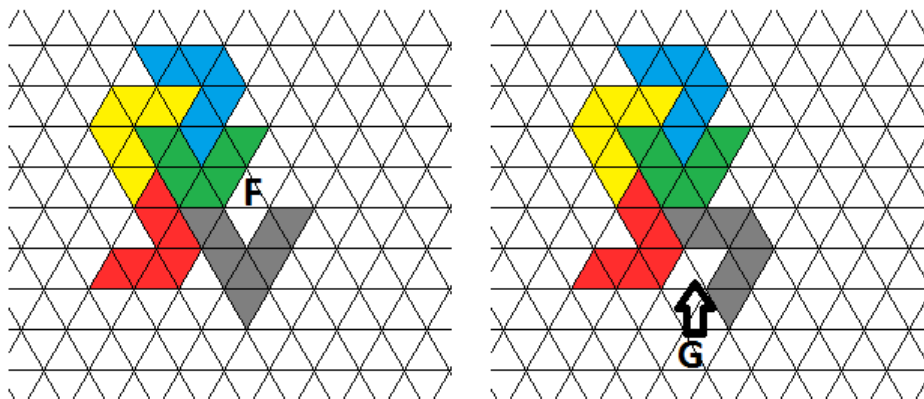


Figure 1.12: Final step.

The 23 heptiamonds left are prototile of monohedral tiling. In this paper we will show the tilings corresponding to some of them, first proving that they indeed admit a monohedral tiling by making use of the Conway Criterion, to proceed then by drawing the tiling.

We can see that the following heptiamond satisfies the Conway Criterion:  $AB$  and  $ED$  are translated copies of each other, while  $BC$ ,  $CD$ ,  $EF$ , and  $FA$  each have centrosymmetry (fig. 1.13).

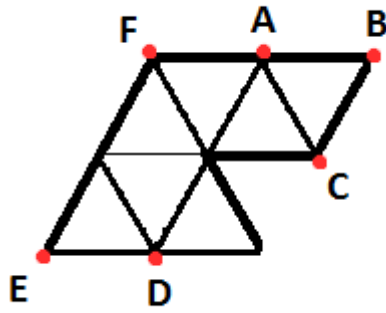


Figure 1.13: One of the 24 heptiamonds.

To obtain the corresponding tiling we just need to stick both of the translated congruent parts ( $AB$  and  $ED$ ) together, and then stick each one of the centrosymmetric parts to itself (fig. 1.14).

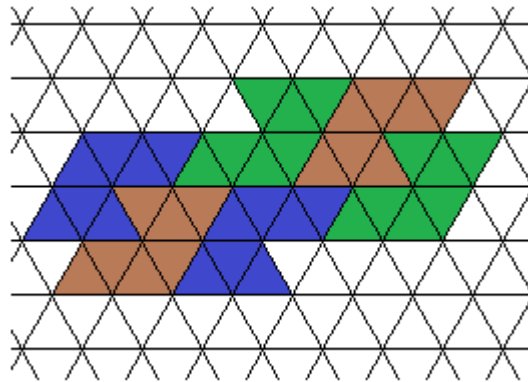


Figure 1.14: The corresponding tiling of the studied heptiamond.

We will now apply the previous procedure to some more heptiamonds to obtain their corresponding tilings (fig. 1.15).

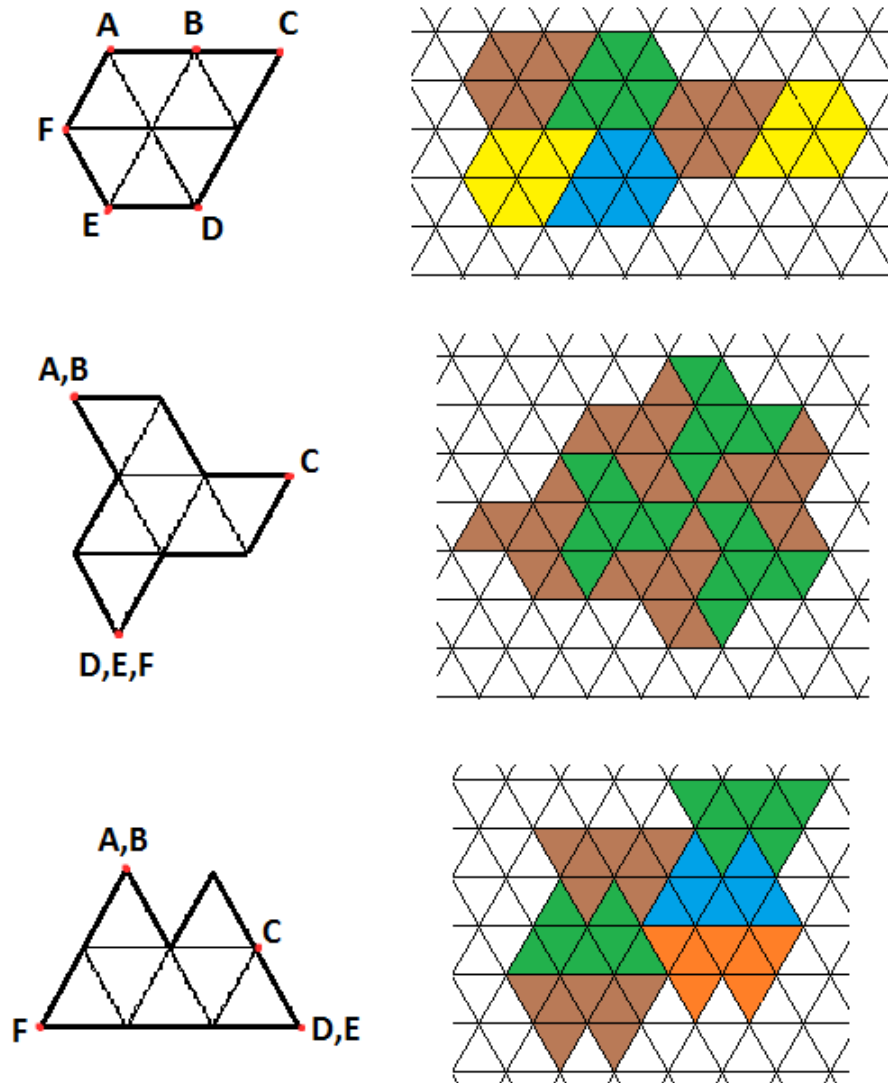


Figure 1.15: Some more examples.

It should be noted that the Conway criterion is a sufficient condition to prove that a piece tiles the plane but not a necessary one. Some pieces do not satisfy the criterion and still tile the plane. In particular, there are two heptiamonds which belong to this group (The third in the first row, and the last in the second row in the fig.1.8). The criterion is useful because such counterexamples are relatively scarce, at least among the small  $n$ -iamonds. In such cases, one can often join a few copies of it together to form a constellation that satisfies the criterion.

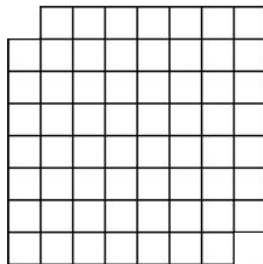
### 1.2.1 Domino Tilings

We have only studied tilings of the plane so far. In this section we will consider tilings of finite regions for the first time, using a "domino" as a prototile in particular. This will serve us as an introduction for the second chapter, in which we will study the Aztec Diamond Theorem, which determines in how many different ways we can tile the aztec diamond (a particular region of the plane) using "dominoes".

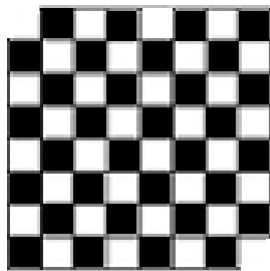
**Definition 1.2.1.** A **domino tiling** is a monohedral tiling with the 2-omino as a prototile. These pieces can tile the plane in infinitely many ways, but our matter of study in this section will be domino tessellation reduced to certain regions of the Euclidean plane.

#### Deciding whether a region admits a domino tiling or not:

Sometimes a parity argument will work to prove that it is not possible to tile a region with domino pieces. For example, consider the case of a rectangle with two of the corners that do not share a side removed:



We can apply a "chess-board" colouring. Since each domino occupies a white square and a black one, and there are  $\frac{n-1}{2}$  white squares and  $\frac{n+1}{2}$  black squares we conclude that this region cannot admit a domino tiling.



This argument will only work for certain regions and in general, more powerful tools are needed. In 1990 William Thurston [18] introduced the concept of "height"

of a tiling and provided us with a test to determine if a simple connected region on the plane, formed by unit squares, can be covered with domino tiles.

The idea of the test is to form an undirected graph with vertices  $(x, y, z)$  in the three-dimensional integer lattice. These points are connected to each other following certain rules related to parity. As a result, the boundary of the region, viewed as a sequence of integer points in the  $(x, y)$  plane, lifts uniquely (once a starting height is chosen) to a path in this three-dimensional graph. A necessary condition for this region to admit a tiling is that this path must close up to form a simple closed curve in three dimensions, however, this condition is not sufficient. Therefore, by means of a more detailed analysis of the boundary path, Thurston gave a criterion that was sufficient as well as necessary.

### Counting domino tilings of different regions:

There is no general method to count the domino tilings for a given region of the two-dimensional lattice. Conversely, different approaches may be useful depending on the region in particular.

One of the most basic cases that one can wonder about is the  $m \times n$  rectangle, which was studied independently by Kasteleyn, Temperley and Fisher [8]. They proved that the number of domino tilings for the  $m \times n$  rectangle is given by:

$$\prod_{j=1}^{\lceil \frac{m}{2} \rceil} \prod_{k=1}^{\lceil \frac{n}{2} \rceil} \left( 4 \cos^2 \frac{\pi j}{m+1} + 4 \cos^2 \frac{\pi k}{n+1} \right). \quad (1.2.1)$$

We should note that when both  $m$  and  $n$  are odd, the formula correctly reduces to zero possible domino tilings. Moreover, Klarner and Pollack showed in 1980 that the sequence reduces to the Fibonacci sequence when tiling the  $2 \times n$  rectangle with  $n$  dominoes (see [9]).

# Chapter 2

## The Aztec Diamond Theorem

This chapter constitutes the main part of this project. We aim to present in detail the alternative proof provided in 2005 [17] by S-P Eu and T-S Fu of the Aztec Diamond Theorem, first proved in 1992 in [1]. Due to the short extension of Eu and Fu’s proof, at first glance it might seem more elementary than previous ones, such as those in [17], but a more careful look raises up the need of side work.

This motivates and justifies our project, and in particular this chapter: our scope is to fill in those “gaps” in [17], presenting a detailed and clarifying exposition of their sketched arguments. In particular, we advance that the main idea is to establish a bijection between the domino tilings of an Aztec diamond and non-intersecting lattice paths.

We start by defining the main object of study:

**Definition 2.0.1.** The **Aztec Diamond** of order  $n$ , denoted by  $AD_n$  (see fig. 2.1), is defined as the union of the unit squares of the lattice  $\mathbb{Z}^2$  with integral corners  $(x, y)$  that satisfy  $|x| + |y| \leq n + 1$ .

Recall that we have defined a domino as a  $1 \times 2$  or  $2 \times 1$  rectangle whose corners are integer numbers, and a domino tiling of a region consists of a cover by a union non-overlapping dominoes. We can then state our theorem:

**Theorem 2.0.2 (Aztec Diamond).** *The number of domino tilings of the Aztec Diamond of order  $n$ ,  $AD_n$  is  $2^{n(n+1)/2}$ .*

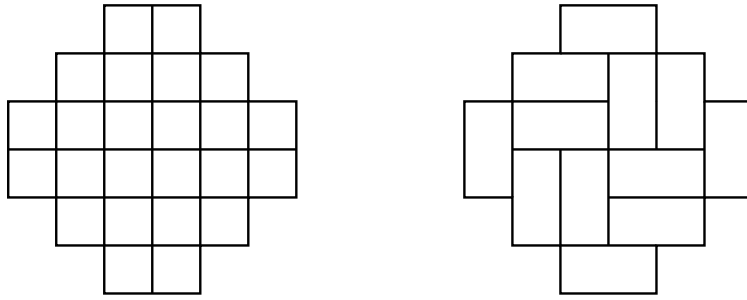


Figure 2.1: On the left, the aztec diamond  $AD_3$ . On the right, a possible domino tiling.

## 2.1 Schröder numbers and Hankel matrices

For each  $n \in \mathbb{N}$  the **large Schröder number**  $S_n$  describes the number of lattice paths in the Cartesian plane that start at  $(0, 0)$ , end at  $(n, n)$ , that never fall below the line  $y = x$ , and are composed only of steps  $(0, 1)$ ,  $(1, 0)$ , and  $(1, 1)$ , i.e.  $\cdot$ ,  $\rightarrow$ ,  $\uparrow$ , and  $\nearrow$ . The first large Schröder numbers are 1, 2, 6, 22, 90, 394, 1806, 8558, 41586, 206098 etc. and are registered in Sloane's Online Encyclopedia of Integer Sequences [19].

Equivalently, Schröder numbers can also refer to the number of paths from  $(0, 0)$  to  $(2n, 0)$ , using only steps  $(1, 1)$ ,  $(1, -1)$ , or  $(2, 0)$  and containing no point below the  $x$ -axis.

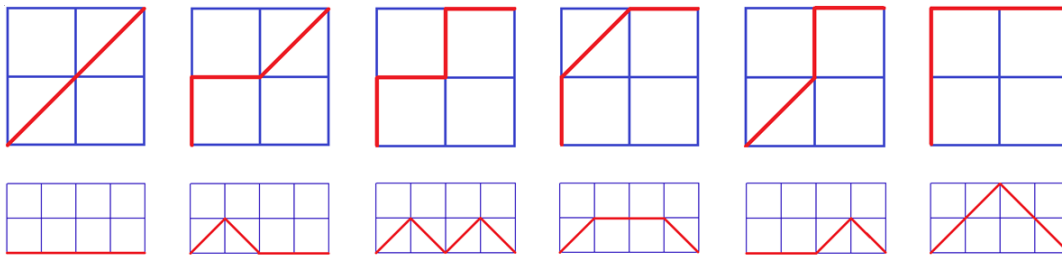


Figure 2.2: In the first row, the paths related to the first definition that generate  $S_2 = 6$ . In the second row, the corresponding paths related to the second definition.

**Lemma 2.1.1.** *The generating function of the large Schröder numbers is*

$$S(x) = \frac{(1-x) - \sqrt{x^2 - 6x + 1}}{2x}. \quad (2.1.1)$$

*Proof.* Consider the second definition. We should first notice that between  $(0, 0)$  and  $(2n, 0)$  the first step is either  $(2, 0)$  or  $(1, 1)$ . If it is the former, we have a Schröder path between  $(2, 0)$  and the first return to the  $x$ -axis. In the second case, if the first

intersection with the  $x$ -axis occurs at  $(2i, 0)$ , we have a Schröder path between  $(1, 1)$  and  $(2i - 1, 1)$ . This yields the recurrence:

$$S_n = \sum_{i=1}^n S_{i-1} \cdot S_{n-i} + S_{n-1} \quad \text{with } n \geq 1, \quad S_0 = 1.$$

Changing indices,

$$S_{n+1} = \sum_{j=0}^n S_j \cdot S_{n-j} + S_n.$$

Taking Generating Functions:

$$\sum_{n \geq 0} S_{n+1} \cdot x^{n+1} = \sum_{n \geq 0} \left( \sum_{j=0}^n S_j \cdot S_{n-j} \right) \cdot x^{n+1} + \sum_{n \geq 0} S_n \cdot x^{n+1}$$

$$S(x) - 1 = xS(x)^2 + xS(x)$$

$$xS(x)^2 + (x - 1)S(x) + 1 = 0.$$

Solving:

$$S(x) = \frac{1 - x \pm \sqrt{x^2 - 6x + 1}}{2x}.$$

We take the negative sign since otherwise the result is not a power series with non-negative powers of  $x$ . □

Similarly, for each  $n \in \mathbb{N}$ , the **small Schröder number**  $s_n$  describes the number of paths from  $(0, 0)$  to  $(2n, 0)$ , using only steps  $(1, 1)$ ,  $(1, -1)$ , or  $(2, 0)$ , containing no point below the  $x$ -axis and no flat step  $(2, 0)$  on the  $x$ -axis. In other words, a small Schröder path is a large Schröder path with no flat steps on the  $x$ -axis. The first small Schröder numbers are 1, 1, 3, 11, 45, 197, 903, 4279, 20793, 103049...

Note that the large and small Schröder are related by a factor 2. We present here two proofs of this fact, the second one provided by the mathematician Ira Gessel relates the number of Schröder paths with at least one flat step on the  $x$ -axis with the number of Schröder paths with no flat steps on the  $x$ -axis.

**Proposition 2.1.2.** *For all  $n \geq 1$   $S_n = 2 \cdot s_n$ .*

*Proof 1.* Let  $(2i, 0)$  be the first return to the  $x$ -axis. Then we have a large Schröder path between  $(1, 1)$  and  $(2i - 1, 1)$ , and a small Schröder path between  $(2i, 0)$  and  $(2n, 0)$ . This yields the recurrence:

$$s_n = \sum_{i=1}^n S_{i-1} \cdot s_{n-i} \quad \text{with } n \geq 1, \quad s_0 = 1.$$

Changing indices,

$$s_{n+1} = \sum_{j=0}^n S_j \cdot s_{n-j}.$$

Taking Generating Functions:

$$\sum_{n \geq 0} s_{n+1} \cdot x^{n+1} = \sum_{n \geq 0} x^{n+1} \left( \sum_{j=0}^n S_j \cdot s_{n-j} \right)$$

$$s(x) - 1 = xS(x)s(x)$$

$$s(x) \cdot (1 - xS(x)) = 1$$

Now using (2.1.2) we get:

$$s(x) = \frac{1 + x - \sqrt{x^2 - 6x + 1}}{4x}$$

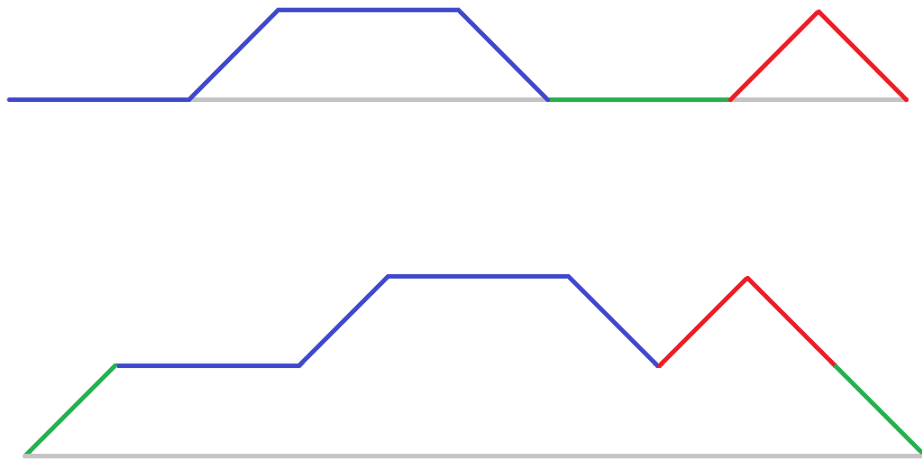
And we can write:

$$S(x) = 2s(x) - 1$$

□

*Proof 2.* We can factor a Schröder path with at least one flat step on the  $x$ -axis as  $PFQ$ , where  $F$  is the last flat step, so  $Q$  has no flat steps on the  $x$ -axis:

We replace the path with  $UPDQ$  where  $U$  is an up step and  $D$  is a down step:



So we have a bijection from Schröder paths with at least one flat step on the

$x$ -axis to small Schröder paths (Schröder paths with no flat steps on the  $x$ -axis). Since Schröder paths are composed by the union of these two sets of paths, the

□

We construct the **Hankel matrices** of the large and small Schröder numbers as follows:

$$H_n := \begin{bmatrix} S_1 & S_2 & \cdots & S_n \\ S_2 & S_3 & \cdots & S_{n+1} \\ \vdots & \vdots & & \vdots \\ S_n & S_{n+1} & \cdots & S_{2n-1} \end{bmatrix}, \quad G_n := \begin{bmatrix} s_1 & s_2 & \cdots & s_n \\ s_2 & s_3 & \cdots & s_{n+1} \\ \vdots & \vdots & & \vdots \\ s_n & s_{n+1} & \cdots & s_{2n-1} \end{bmatrix}.$$

The reason for defining these matrices is that as we shall see in Section 2.3, is that their determinants will agree with the with the numbers of  $n$ -tuples of non-intersecting large and small Schröder paths, respectively.

## 2.2 Bijection between tilings and paths

The goal of this section is to prove that there exists a bijection between domino tilings of the Aztec Diamond and tuples of Schröder paths. We start by defining the sets of Schröder paths that we are going to relate the tilings to.

For this purpose, we associate an  $n$ -tuple of non-intersecting paths to each domino tiling in the following way:

Given a tiling  $\mathcal{T}$  of  $AD_n$ , let the rows of  $AD_n$  be indexed from bottom to top, we take the ones in the bottom half (from 1 to  $n$ ). For each, we define a path  $p_i$  ( $1 \leq i \leq n$ ) from the center of the left-hand edge of the  $i$ -th row to the center of the right-hand edge of the  $i$ -th row. The steps are formed by joining an edge of a domino tile  $T_1$  with another edge of  $T_1$ , in such a way that the path passes trough the center of  $T_1$ , that is, the step is symmetric with respect to the center of  $T_1$ . This way, we have associated an  $n$ -tuple  $(p_1, p_2, \dots, p_n)$  of non-intersecting paths to each tiling (fig. 2.3). We denote the set of such  $n$ -tuples by  $\mathcal{P}_n$

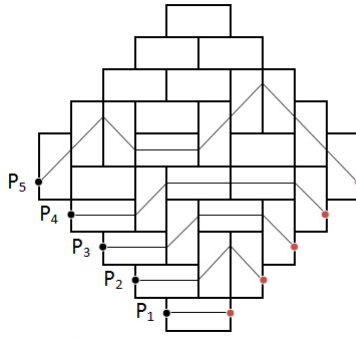


Figure 2.3: A domino tiling of  $AD_5$  with its associated  $n$ -tuple of paths.

It is remarkable that the paths related to the Aztec Diamond are very similar to Schröder paths. We will now introduce some definitions that will help us to determine which are exactly the properties of these paths.

**Definition 2.2.1.**  $\mathcal{R}_n$  (resp.  $\mathcal{Q}_n$ ) denotes the set of  $n$ -tuples  $(r_1, r_2, \dots, r_n)$  of large (resp. small) Schröder paths satisfying the following two conditions:

(C1) Each path  $r_i$  goes from  $(-2i + 1, 0)$  to  $(2i - 1, 0)$  for  $1 \leq i \leq n$ .

(C2) Any two paths  $r_i$  and  $r_j$  do not intersect.

We note that (C1) and (C2) imply that each  $r_i$  has  $i$  up steps at the beginning and  $i$  down steps at the end.

We will now establish a bijection  $\psi: \mathcal{P}_n \rightarrow \mathcal{R}_n$ , which sends  $(p_1, p_2, \dots, p_n)$  to  $(r_1, r_2, \dots, r_n)$ , where  $r_i$  is obtained by adding  $i$  up steps at the beginning of  $p_i$  and  $i$  down steps at the end (fig. 2.4).

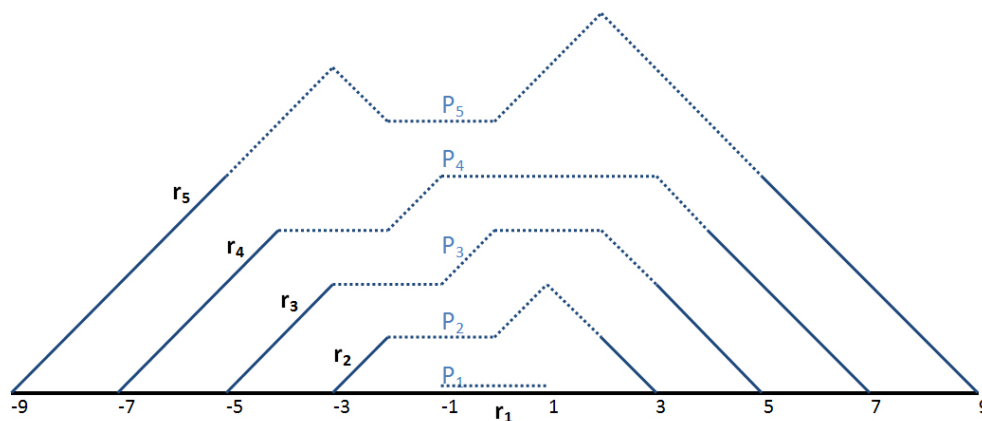


Figure 2.4: The corresponding  $n$ -tuples of paths to the tiling of the Figure 2.3

Conversely,  $\psi^{-1}$  of a given  $(r_1, r_2, \dots, r_n)$  is the path obtained by removing  $i$  up steps at the beginning of  $r_i$  and  $i$  down steps at the end.

It is obvious that for each tiling there only exists a unique associated tuple. However, the inverse is not that trivial, and it was not proved in the original paper [17], so we will prove it here.

We first need to introduce two different distances.

**Definition 2.2.2.** The **distance** between two paths (or tiles) at the  $i$ -th column is the vertical distance between the two paths (or tiles) measured between the centers of the squares that intersect with the paths (or tiles) at that column (fig. 2.5).

We say that two paths are **adjacent** at  $i$  if the distance between them at the  $i$ -th column is no greater than 2, so one can check that no tile would fit in between the paths at that column.

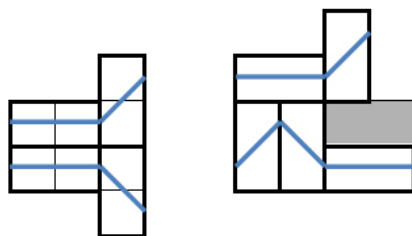


Figure 2.5: On the left, the distance between the paths is 1 at the first two columns and 2 at the last column. On the right, the distance at the last column is 2.5, greater than 2, and a domino fits in between.

**Definition 2.2.3.** The **boundary distance** between two paths at the  $i$ -th column is the vertical distance between the two paths measured between the intersections of each path with the vertical line next to the right to the  $i$ -th column (fig. 2.6).

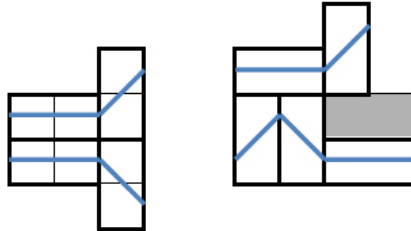


Figure 2.6: On the left, the boundary distance between the paths is 1 at the first two columns and 3 at the last column. On the right, the boundary distance is 1 at the first column, 2 at the second, and 3 at the third.

**Lemma 2.2.4.** *There cannot be two paths at boundary distance 1 at the  $i$ -th column that complete a full step at that column, that is, one of them must have the beginning of a flat step at that column. In other words, if two paths are at boundary distance 1 at the  $i$ -th column, exactly one of them will have a flat step contained in the  $i$ -th and  $(i + 1)$ -th column.*

*Proof.* For the sake of a contradiction we assume that there exist two paths  $p_u$  and  $p_l$  (upper and lower) at boundary distance 1 at the  $i$ -th column which finish a step at that column.

We denote the number of up, down and flat steps of  $p_u$  until the  $i$ -th column as  $u$ ,  $d$ ,  $f$  respectively, and analogously  $u'$ ,  $d'$ ,  $f'$  for  $p_l$ .

If we consider a virtual square on the left to  $p_l$ , with half a flat step on it, so both paths start at the same column, the distance at the beginning of the two paths is already 1, so up to this point, the variation in height of both  $p_u$  and  $p_l$  has been the same. Thus,

$$u - d = u' - d'. \quad (2.2.1)$$

On the other hand, the horizontal length travelled by  $p_u$  overcomes the one travelled by  $p_l$  by 1. Thus,

$$2h + u + d = 2h' + u' + d' + 1. \quad (2.2.2)$$

Joining the two conditions, we get

$$2h + 2d = 2h' + 2d' + 1. \quad (2.2.3)$$

Since all the variables are natural numbers, the left hand side is even, while the right hand side is odd. This yields a contradiction.

□

**Lemma 2.2.5.** *Given two adjacent paths  $p_u$  and  $p_l$  at the  $i$ -th column, the distance at the  $(i + 1)$ -th column can only increase in one of the following ways:*

I) *From 1 to 1.5.*

II) *From 1.5 to 2, 2.5 or 3.*

III) *From 2 to 2.5 or 3.*

*Proof.* In the case I), both  $p_u$  and  $p_l$  have a flat step or horizontal domino at the  $i$ -th column. However, they cannot share a full side, since this would contradict 2.2.4. The only possible increase is by 0.5 then (fig. 2.7).

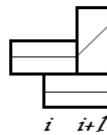


Figure 2.7: Increase corresponding to I) excluding isometries.

The case II) occurs when one of the paths presents a vertical domino at the  $i$ -th column, while the other path presents a horizontal one. The three possible increases in distance are 0.5, 1 or 1.5 (fig. 2.8).

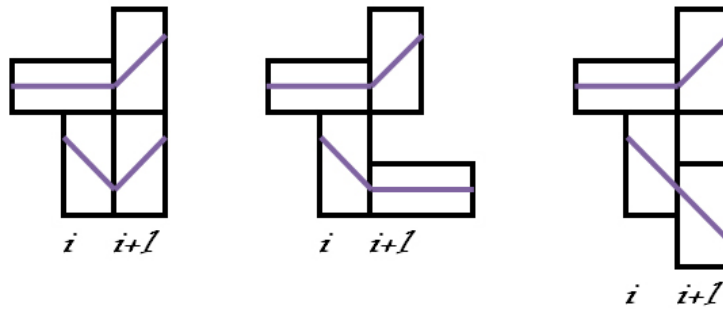


Figure 2.8: Increases corresponding to II) excluding considering isometries.

We note that although in the third possibility the distance between the paths is 3 at the  $(i + 1)$ -th column, a vertical domino does not fit in the space between the paths. This would only happen with distance 3 if both  $p_u$  and  $p_l$  presented a horizontal domino at this column (fig. 2.9), which is not the case.

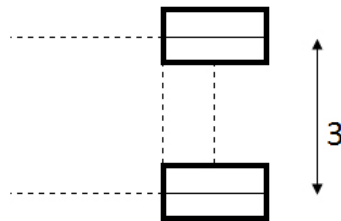


Figure 2.9: The only case with distance 3 in which a vertical domino fits in between.

Finally, the case III) occurs when both  $p_u$  and  $p_l$  have a vertical domino at the  $i$ -th column. Moreover, both paths must be parallel at this column, provided that the opposite would contradict 2.2.4 (fig. 2.10).

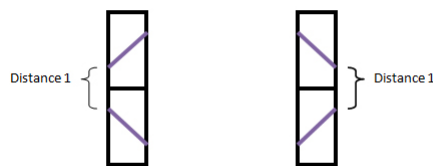


Figure 2.10: The two different cases that would contradict 2.2.4.

□

Then, the only possible increases are by 0.5 or 1 (fig. 2.11). It should be noticed that once again the case with distance 3 does not admit a vertical domino in between.

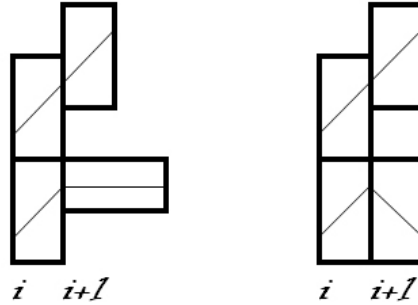


Figure 2.11: Increases corresponding to III) excluding isometries.

**Proposition 2.2.6.** *There is a unique domino tiling  $\mathcal{T}$  that corresponds to a given  $n$ -tuple  $(p_1, p_2, \dots, p_n)$  of paths.*

*Proof.* The squares that are crossed by a path can only be tiled in a unique way, provided that each step of the path determines a unique position for the domino that covers that square.

On the other hand, we are now going to show that the squares that are not crossed by any path also admit a unique possibility, consisting of a covering by only dominoes in a horizontal position.

When the distance of two adjacent paths at the  $i$ -th column  $p_u$  and  $p_l$  increases at the  $(i+1)$ -th column, it will always be in such a way that the space originated between  $p_u$  and  $p_l$  at that column will not be enough for a vertical domino to fit (lemma 2.2.5). Conversely, it will only allow a horizontal domino or will remain small enough so no domino can fit.

When filling the region between  $p_u$  and  $p_l$  we do it from left to right. Let  $i$ -th be the first column at which the distance between the paths is equal or greater to 2.5. The first tile we put in order to cover the region between paths must be in a horizontal position, occupying the  $i$ -th and  $(i+1)$ -th columns (see fig.2.12).

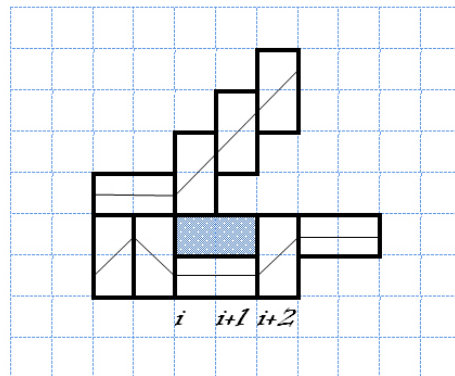


Figure 2.12: As in the example, the covering should start from the left.

We can now consider the new tile as the section of a path, a flat step  $s_f$ . To cover the spaces between  $p_u$  and  $p_l$  at the  $(i+1)$ -th column we consider the distance between  $p_u$  and  $s_f$ , and the distance between  $s_f$  and  $p_l$  at the  $(i+1)$ -th column. Since the two pairs  $p_u$  and  $s_f$  are adjacent at the  $i$ -th column and the same occurs regarding  $s_f$  and  $p_l$ , these two distances cannot be greater than 3, and no vertical domino will fit between  $p_u$  and  $s_f$ , or  $s_f$  and  $p_l$ , at the  $(i+1)$ -th column (lemma 2.2.5). This way, the spaces at the  $(i+1)$ -th column (if they exist) can only be covered by horizontal tiles (see fig. 2.13)

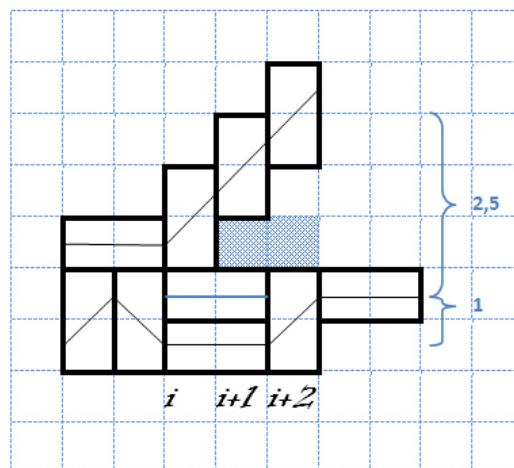


Figure 2.13: In this example the distance at the  $(i+1)$ -th column between  $p_f$  and  $p_l$  is only 1, so no domino fits in between. However, the distance between  $p_u$  and  $s_f$  is 2, so a domino fits in between, but only in a horizontal position .

We can repeat this process and it will come to an end, since the region between

paths and the Aztec Diamond itself are finite. All the regions between paths will be then uniquely covered by horizontal dominoes, while the rest of the tiles will be determined by the shape of the paths.

Finally, it should be remarked that the region above the upper path  $P_n$  of the Aztec Diamond  $AD_n$  can also be considered a region between paths, so it can only be covered by horizontal dominoes. It is enough to create a virtual path composed by two segments, intersecting all the vertices of the upper side of  $AD_n$  (see fig. 2.15).

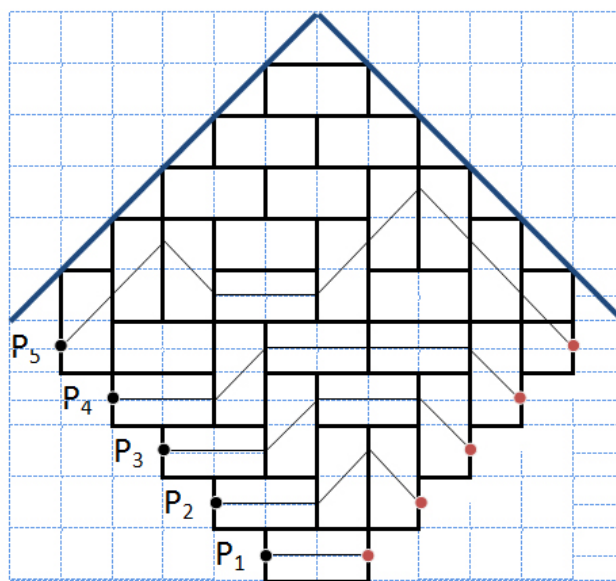


Figure 2.14: An example of the virtual path for a tiling of  $AD_5$ .

□

As a result, we have built a bijection between the number of domino tilings of the Aztec Diamond to  $\mathcal{R}_n$ , the set of families of Schröder paths satisfying (C1) and (C2).

**Corollary 2.2.7.** *The number of domino tilings of the Aztec Diamond  $AD_n$  equals the number of  $n$ -tuples of  $\mathcal{R}_n$ .*

## 2.3 Hankel matrices and $n$ -tuples of Schröder paths

We start recalling some basic definitions:

**Definition 2.3.1.** A **permutation** is a bijection of the set  $\{1, \dots, n\}$  onto itself:

$$\sigma : \{1, \dots, n\} \longrightarrow \{1, \dots, n\}$$

$$(123 \cdots n) \rightsquigarrow (z_1 z_2 \cdots z_n).$$

Given a permutation  $\sigma$ , its number of **inversions** is

$$\text{inv}(\sigma) := \text{Card}\{(z_i, z_j) \mid i < j \text{ and } z_i > z_j\},$$

and we define its **sign** as  $\text{sign}(\sigma) := (-1)^{\text{inv}(\sigma)}$ .

Using the technique of a sign-reversing involution over a signed set, we prove that the cardinalities of  $\mathcal{R}_n$  and  $\mathcal{Q}_n$  (recall Def. 2.2.1) agree with the determinants of  $H_n^{(1)}$  and  $G_n^{(1)}$ , respectively.

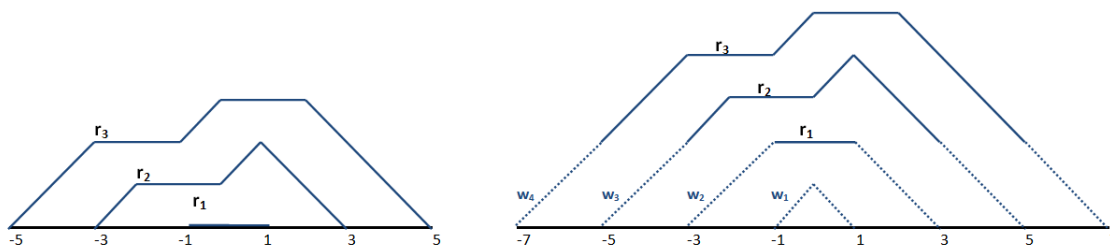
The idea of such technique is the following: recall that an **involution** is a function  $f$  that is its own inverse, that is,  $f(f(x)) = x$ . If we define a sign-reversing involution on a signed set  $P$ , it has to occur that outside the fixed points, all other positive points are mapped to the negative ones and viceversa, and thus is a bijection between that two sets. Therefore the difference between the cardinals of the positive points  $P^+$  and negative ones  $P^-$  is given by the number of fixed points of the involution.

Let us see this: suppose that there exists a sign-reversing involution  $\psi$  defined on  $P$ . For each  $p \in P^+$  not fixed there exists  $q \in P^+$  such that  $\psi(p) = q$  and  $p = \psi(\psi(p)) = \psi(q)$ , and thus  $|P^+ \setminus \{\text{fixed points of } \psi\}| = |P^-|$ , which leads to

$$|P^+| - |P^-| = |\{\text{fixed points of } \psi\}|. \quad (2.3.1)$$

Before we start, it should also be noticed that there is an immediate bijection  $\phi$  between  $\mathcal{R}_{n-1}$  and  $\mathcal{Q}_n$  for  $n \geq 2$ . It sends  $(r_1, \dots, r_{n-1}) \in \mathcal{R}_{n-1}$  to  $\phi((p_1, \dots, p_{n-1})) = (q_1, \dots, q_n) \in \mathcal{Q}_n$ , where  $q_1$  is an up step followed by a down step, and for  $i \geq 2$ ,  $q_i$  is obtained from  $p_{i-1}$  by attaching 2 up steps at the beginning and 2 down steps attached at the end, so it rises above the  $x$ -axis), for  $2 \leq i \leq n$  (see fig. ??). Hence, for  $n \geq 2$ , we have

$$|\mathcal{R}_{n-1}| = |\mathcal{Q}_n|. \quad (2.3.2)$$

Figure 2.15: An example of the bijection between  $\mathcal{R}_{n-1}$  and  $\mathcal{Q}_n$ .

**Proposition 2.3.2.** For  $n \geq 1$ , we have

$$(i) |\mathcal{R}_n| = \det(H_n) = 2^{n(n+1)/2}, \text{ and}$$

$$(ii) |\mathcal{Q}_n| = \det(G_n) = 2^{n(n-1)/2}.$$

*Proof.* For  $1 \leq i \leq n$ , let  $A_i$  be the point  $(-2i+1, 0)$ ,  $B_i$  denote the point  $(2i-1, 0)$ , and  $h_{ij}$  denote the  $(i, j)$ -entry of  $H_n$ . Observe that  $h_{ij} = S_{i+j-1}$  is equal to the number of large Schröder paths from  $A_i$  to  $B_j$ . The reason for this is that the segment  $[(-2i+1, 0), (2i-1, 0)]$  is just a translation of the interval  $[(0, 0), 2(i+j-1, 0)]$ .

Let  $P$  be the set of ordered pairs  $(\sigma, (t_1, \dots, t_n))$ , where  $\sigma$  is a permutation of  $\{1, \dots, n\}$ , and  $(t_1, \dots, t_n)$  is an  $n$ -tuple of large Schröder paths such that  $t_i$  goes from  $A_i$  to  $B_{\sigma(i)}$ . According to the sign of  $\sigma$ , we can partition the pairs in  $P$  into the sets  $P^+$  and  $P^-$ . Then, by definition of determinant we have

$$\det(H_n^{(1)}) = \sum_{\sigma \in \mathcal{S}_n} \text{sgn}(\sigma) \prod_{i=1}^n h_{i, \sigma(i)} = |P^+| - |P^-|.$$

Therefore, if we are able to define a sign-reversing involution  $\psi$  on  $P$ , then by equation (2.3.1)  $\det(H_n)$  will be equal to the number of fixed points of  $\psi$ .

Let  $(\sigma, (t_1, \dots, t_n)) \in P$  be a pair that contains at least two paths of  $(t_1, \dots, t_n)$  intersect. We choose the first pair  $i < j$  in lexicographical order such that  $t_i$  intersects  $t_j$ . Then, we can construct new paths  $t'_i$  and  $t'_j$  by switching the tails after the last point of intersection of  $t_i$  and  $t_j$ .

Observe that  $t'_i$  goes from  $A_i$  to  $B_{\sigma(j)}$  and  $t'_j$  goes from  $A_j$  to  $B_{\sigma(i)}$ . Since  $\sigma \circ (ij)$  maps  $i$  to  $\sigma(j)$  and  $j$  into  $\sigma(i)$ , and  $k$  into  $\sigma(k)$ , for  $k \neq i, j$ , we can define

$$\psi((\sigma, (t_1, \dots, t_n))) = (\sigma \circ (ij), (t_1, \dots, t'_i, \dots, t'_j, \dots, t_n)).$$

Clearly,  $\psi$  is sign-reversing. Since the first intersecting pair  $i < j$  is not affected by  $\psi$ ,  $\psi$  is an involution. The fixed points of  $\varphi$  are the pairs  $(\sigma, (t_1, \dots, t_n)) \in P$  such that  $\sigma$  is the identity, and  $t_1, \dots, t_n$  do not intersect, i.e.,  $(t_1, \dots, t_n) \in \mathcal{R}_n$ . Hence  $\det(H_n) = |\mathcal{R}_n|$ . Similarly, we have  $\det(G_n) = |\mathcal{Q}_n|$ . It follows from 2.3.2, that is, the bijection constructed in the previous section between  $\mathcal{R}_{n-1}$  and  $\mathcal{Q}_n$ , and the fact  $H_n^{(1)} = 2G_n^{(1)}$  that

$$|\mathcal{R}_n| = \det(H_n) = 2^n \cdot \det(G_n) = 2^n |\mathcal{Q}_n| = 2^n |\mathcal{R}_{n-1}|.$$

Note that  $|\mathcal{R}_1| = 2$ , and hence, by induction, the statement holds.  $\square$

# Conclusion and generalizations

On this document, we have started introducing tilings and tessellations, along with some of the most relevant results related to them. We have tried to expose them in a general revision, that can be applied later onto particular cases. For example, we have shown how to apply Conway Criterion to heptiamonds.

Conversely, in Chapter 2 we have followed a different approach. Instead of presenting a general review of concepts, we have focused on a particular topic: the Aztec Diamond Theorem. Nonetheless, the methods and techniques appearing on its proof can also be applied to other settings, as when studying tilings over other regions of the plane  $\mathbb{R}^2$  or other areas of combinatorics and graph theory. In particular, the technique of computing the number of non-intersecting paths with the determinant of a matrix is very popular (called the Gessel-Viennot lemma).

## Variations of the Aztec Diamond

The number of tilings of a region can vary a lot even with small changes over the original region, and this is also the case with the Aztec Diamond.

If the regular Aztec Diamond  $AD_n$  is replaced by the **augmented Aztec Diamond** (see fig. 2.16) of order  $n$  with 3 long rows in the middle rather than 2, the number of tilings drops to the much smaller number  $D(n, n)$ , a Delannoy number, which has only exponential rather than super-exponential growth in  $n$ . For the **reduced Aztec Diamond** (see fig. 2.16) of order  $n$  with only one long middle row, there is only one tiling.

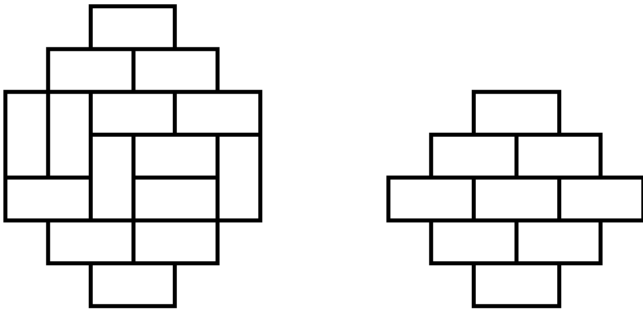


Figure 2.16: On the left, the augmented Aztec Diamond of order 3 with one possible domino tiling . On the right, reduced Aztec Diamond of order 3 with its unique possible domino tiling.

# Bibliography

- [1] **N. Elkies, G.Kuperberg, M.Larseb, and J.Prop** Alternating-sign matrices and domino tilings (Part 1), *J. Algebraic Combinatorics* 1, 111-132, 1932. [15](#)
- [2] **D .Ellard** Poly-iamond enumeration. *Math. Gazzete* 66, 310-314, 1982. [7](#)
- [3] **I. M. Gessel** [www.crm.umontreal.ca/CanaDAM2009/pdf/gessel.pdf](http://www.crm.umontreal.ca/CanaDAM2009/pdf/gessel.pdf) *Department of Mathematics, Brandeis University*.
- [4] **S. W. Golomb** Polyominoes (second edition), Princeton University Press, 1994.
- [5] **B. Grünbaum and G. C. Shephard** *Tilings and Patterns*, 1987, pp.474-489. [5](#)
- [6] **H. Heesch** Aufbau der Ebene aus kongrueten Bereichen. *Nachr.Ges.Wis.Göttingen*, New Ser,1 (1935) 115-117. [5](#)
- [7] **D. Hilbert** Mathematische Probleme. *Göttinger Nachrichten* 1900, pp.253-297. [5](#)
- [8] , **P. W. Kasteleyn** The statistics of dimers on a lattice. I. The number of dimer arrangements on a quadratic lattice, *Physica* 27 (12): 1209–1225, 1961. [14](#)
- [9] , **D. Klarner and J.Pollack** Domino tilings of rectangles with fixed width. *Discrete Mathematics* Vol. 32, pp. 45-52. [14](#)
- [10] **W. F. Lunnon** Counting polyominoes. *Computers in Number Theory*, 347-372,1971. [7](#)
- [11] **W. F. Lunnon** Counting hexagonal and triangular polyominoes. *Graph Theory and Computing*, 87-100, 1971. [7](#)
- [12] **G. E. Martin** Polyominoes: A guide to puzzles and problems in tiling, Mathematical Association of America, 1991 (second edition, 1996).

- 
- [13] **J. Myers** Polyamino, polyhex and polyiamond tiling, <https://www.polyomino.org.uk/mathematics/polyform-tiling/> 8
- [14] **I. Niven** *The American Mathematical Monthly* Vol.85, No.10 (Dec.,1978), pp.785-792 7
- [15] **K. Reinhardt** (1928). Zur Zerlegung der euklidischen Räume in kongruente Polytope. *Sitzungsberichte der Preussischen Akademie der Wissenschaften Berlin, Physikalisch-Mathematische Klasse* 150–155. 7
- [16] **D. Schattschneider** Tiling the plane with congruent pentagons. *Mathematics Magazine*, Vol 51. 29-44, 1978.
- [17] **Sen-Peng Eu and Tung-Shan Fu** A simple proof of the Aztec diamond theorem. *Electron. J. Combin.*, 12:Research Paper 18, 8 2005. 15, 21
- [18] **W. Thurston** Conway's Tiling groups. *The American Mathematical Monthly.*, Vol. 97, No. 8, pp.757-773 1990. 13
- [19] <https://oeis.org/A006318>. 16